

Online EV Charge Scheduling Based on Time-of-Use Pricing and Peak Load Minimization: Properties and Efficient Algorithms

Weitiao Wu^{ID}, Yue Lin, Ronghui Liu, Yaohui Li, Yi Zhang, and Changxi Ma^{ID}

Abstract—Electric vehicles (EVs) endow great potentials for future transportation systems, while efficient charge scheduling strategies are crucial for improving profits and mass adoption of EVs. Two critical and open issues concerning EV charging are how to minimize the total charging cost (Objective 1) and how to minimize the peak load (Objective 2). Although extensive efforts have been made to model EV charging problems, little information is available about model properties and efficient algorithms for dynamic charging problems. This paper aims to fill these gaps. For Objective 1, we demonstrate that the greedy-choice property applies, which means that a globally optimal solution can be achieved by making locally optimal greedy choices, whereas it does not apply to Objective 2. We propose a non-myopic charging strategy accounting for future demands to achieve global optimality for Objective 2. The problem is addressed by a heuristic algorithm combining a multi-commodity network flow model with customized bisection search algorithm in a rolling horizon framework. To expedite the solution efficiency, we derive the upper bound and lower bound in the bisection search based on the relationship between charging volume and parking time. We also explore the impact of demand levels and peak arrival ratios on the system performance. Results show that with prediction, the peak load can converge to a globally optimal solution, and that an optimal look-ahead time exists beyond which any prediction is ineffective. The proposed algorithm outperforms the state-of-the-art algorithms, and is robust to the variations of demand and peak arrival ratios.

Index Terms—Electric vehicle, online charging, time-of-use pricing, peak load, prediction, heuristic.

I. INTRODUCTION

WITH the increasing penetration of electric vehicles, the charging demand will dramatically increase at charging stations [1]. Since the parking time of a vehicle usually accounts for more than 90% of a day [2], parking lots have

Manuscript received November 8, 2019; revised May 20, 2020; accepted July 15, 2020. Date of publication September 2, 2020; date of current version December 28, 2021. This work was supported in part by the Science and Technology Program of Guangzhou, China, under Project 201904010202, in part by the National Science Foundation of China under Project 61703165, Project 71890972, and Project 71890970, and in part by the U.K. Department for Transport (Project “Future Streets”). The Associate Editor for this article was S. E. Li. (*Corresponding author: Weitiao Wu*)

Weitiao Wu, Yue Lin, Yaohui Li, and Yi Zhang are with the School of Civil Engineering and Transportation, South China University of Technology, Guangzhou 510641, China (e-mail: ctwtwu@scut.edu.cn).

Ronghui Liu is with the Institute for Transport Studies, University of Leeds, Leeds LS2 9JT, U.K.

Changxi Ma is with the School of Traffic and Transportation, Lanzhou Jiaotong University, Lanzhou 730070, China.

Digital Object Identifier 10.1109/TITS.2020.3014088

played an important role for charging EVs, especially for workplaces, shopping centers and entertainment areas. The high penetration of EVs will have a significant impact on the electric grid. In particular, uncoordinated EV charging will result in an increase in charging costs and system peak loads.

According to the time-of-use (TOU) electricity price, the pricing in peak hours is approximately two or three times of that in off-peak hours. In the context of TOU pricing, the charging schedule has a great impact on charging costs. Generally, the parking time (e.g., duration of working hours) is longer than the minimum required charging time. This provides opportunities for commercial aggregators or charging service providers to charge EVs flexibly to reduce the energy procurement costs and maximize their profit. Therefore, one of the problems is how to coordinate EV charging so as to minimize the total charging cost. On the other hand, uncoordinated EV charging would increase the peak-time demand and overload the grid, which imposes higher strains on the generation units and transmission and distribution systems. This may lead to unexpected voltage drops and poor power quality [3]–[5]. To ensure a level of operational security, more costly peaking generators are required to overcome the challenges of peaking power needs. Therefore, another critical issue for EV charging is how to reduce the peak load. The purpose of this paper is to address dynamic EV charging problems with two aforementioned objectives: (1) minimizing the total charging cost; and (2) minimizing the peak load. With regard to Objective 2, two schemes are studied depending on whether the anticipated future vehicle arrivals are taken into account.

The successful large-scale implementation of dynamic EV charging largely depends on developing efficient solution algorithms. Tang *et al.* (2016) [6] provided an overview of online EV charge scheduling algorithms under various conditions and highlighted the importance of future data. From the modeling perspective, the dynamic charging schedule problem has a more complex structure than the respective static versions. Unlike the static versions, in the dynamic counterpart, the arrival times and charging information of the vehicles are not known in advance. A common solution to handle the dynamic variant is to construct a sequence of instances in a rolling horizon framework, where each sequence is treated as a static problem. However, this would greatly increase computational burden and hinder the implementation

of a real-time optimal charging solution, especially when the number of instances is sufficiently large. Therefore, a critical challenge to address the dynamic charging problem is how to achieve globally optimal solution in a reasonable amount of time. Although a variety of intelligent algorithms have been proposed in the literature [7], little evidence is provided about the model properties and efficient algorithms for dynamic charging problems. It is well recognized that the greedy algorithm, though it will not necessarily achieve a global optimum, is more advantageous in terms of computational efficiency than other algorithms since it only makes a locally optimal choice at each stage. A problem is characterized by the greedy-choice property if a globally optimal solution can be achieved by making locally optimal choices. In other words, we can make whatever choice seems best at the moment and then solve the subproblems that arise later. In this way, the computational efficiency could be improved significantly.

Previous studies on EV charge scheduling optimization have not investigated the greedy-choice property, which limits the improvement of algorithm's efficiency and operational flexibility. Meanwhile, the collective effects of coordinated charging control are closely related to the traffic demand, while in practice the mobility patterns and traffic conditions are very complex. With an expectation that a variety of factors (e.g., charging demand, arrival patterns) may exert an influence on the charging system, there is an imminent need to comprehensively evaluate how these factors affect the system performance, such as algorithmic efficiency and energy savings. Such an understanding is important for the design optimization of human-energy-mobility systems. This paper aims to fill the aforementioned methodological gaps and assess the impacts.

The remainder of the paper is organized as follows. In the next section, literature review is given. In Section III, the model formulations, model properties and solution algorithms are provided. Section IV performs experiments to verify the effectiveness of our models. Finally, Section V provides conclusions and future works.

II. LITERATURE REVIEW

Generally, EV charging strategies can be divided into two categories: decentralized strategies and centralized strategies. In the former strategy, EV owners can determine the charging time and power. The network operator can impose certain price incentives to achieve peak shaving and valley infilling [8]–[10]. Although EV owners are provided with more flexibility under such a strategy, the solutions may not be optimal from a system perspective. For the centralized strategy, the aggregator or service provider determines the charging schedule for all EVs to achieve an optimal system.

With respect to the objectives, some efforts were made to minimize the total cost and maximize the profit of operators, while the others focused on reducing the peak load and grid congestion by filling the valleys. He *et al.* [11] proposed both globally and locally optimal scheduling schemes for EV charging and discharging, in an aim to minimize the total cost. Sundstrom and Binding [12] optimized the charging plan to avoid distribution grid congestion considering the

imperatives of EV owners. Maigha and Crow [4] investigated the charging coordination for valley filling and charging cost reduction. Bandpey and Firouzjah [13] presented a two-stage charging strategy for plug-in electric vehicles to reduce the load peak considering the nonlinear dynamic behavior of batteries. Robu *et al.* (2013) [14] developed an online resource allocation method and applied it to EV charging, where the agents need to report the marginal valuation function and maximum consumption rate upon arrival. Jian *et al.* [15] developed an efficient valley-filling strategy for centralized coordinated charging for large-scale EVs. Alinia *et al.* (2019) [16] developed a social welfare maximization problem for online EV charge scheduling with the charging station capacity and uncertain EV arrivals, considering the on-arrival commitment and group-strategy-proofness. Yang *et al.* [17] investigated the charge scheduling optimization problem for a wirelessly charged electric bus system, with the objective to minimize the operating electricity cost. Zhang *et al.* [18] investigated delay-optimal charge scheduling for a charging station under long-term cost constraint. Ammous *et al.* [19] considered joint delay and cost optimization of on-demand EV charge scheduling.

There is also some literature that investigates the use of multi-objective optimization to make the trade-offs between different interests. Kang *et al.* [20] presented an EV charging scheduling system with the objective of minimizing negative impacts to the power grid while meeting the users' charging requirements. Zakariazadeh *et al.* [21] considered both minimization of total operational costs and emissions in the charging scheduling problem. Zhan *et al.* [22] proposed a decentralized method to schedule EV charging loads to fill load valleys. Hajforoosh *et al.* [5] proposed algorithms that minimize the costs with related to energy generation and grid losses while maximizing the power delivered to EVs. Wu *et al.* [23] proposed a battery swapping station model to determine the optimal charging scheme for incoming batteries, with the objective of maximizing the battery stock level in the station and minimizing the average charging damage. In addition to charging scheduling problems from the supply side, there also exist a handful of works on the management of power systems through economic incentives (e.g., adaptive pricing) and charging behavior from the demand side. For example, Zhang *et al.* [24] proposed a pricing scheme to minimize the service dropping rate of charging stations via queuing theory.

The mass adoption of online EV charging largely depends on the efficiency of solution algorithms. However, a critical issue of previous studies on EV charge scheduling optimization is that the greedy-choice property has not been investigated, which hinders the improvement of the algorithm efficiency and operational flexibility. In addition, how traffic conditions (e.g., charging demand, arrival patterns) exert influence on the system performance remains unclear. Distinctly from prior research, we investigate the model properties for these two objectives in dynamic charging problems. commendably, we further propose efficient algorithms based on the theoretical properties, enabling the models' applicability in large-scale scenarios. We also investigate the impact of

traffic conditions (e.g., charging demand, arrival patterns) on the system performance. This research is expected to provide managerial insights for efficient coordinated charging control.

To summarize, the contributions of our study include, but are not limited to:

- We prove that in the ordinary sense, the dynamic charging problem with Objective 1 has the greedy-choice property that a globally optimal solution can be assembled by making locally optimal greedy choices, whereas the problem with Objective 2 cannot achieve global optimality with greedy choices.
- To achieve global optimality with Objective 2, we propose a non-myopic charging model accounting for anticipated future charging requests. The model is addressed by a heuristic algorithm that combines a multi-commodity network flow model with a customized bisection search algorithm in a rolling horizon framework. In particular, we derive a set of valid inequalities for the bisection search algorithm to expedite the solution speed.
- We conduct extensive numerical experiments to test the performance of our solution approach and derive significant managerial insights. In particular, our results show the following:

-The demand levels and peak arrival ratios considerably affect the system performance.

-With the non-myopic prediction-based strategy, the peak load can converge to the global optimal solution, and there is an optimal look-ahead time beyond which the improvement of any prediction is trivial.

-The algorithm efficiency is quite good and robust to the variations of demand and peak arrival ratios.

-The prediction-based strategy is robust to prediction uncertainty particularly under a high peak arrival ratio, which is very applicable to workplace charging which features commuting demand.

III. MODEL DEVELOPMENT

A. Problem Description

With the summary of notations in Table I, we present the system model. We consider a time-slotted system model where the time horizon is divided into a number of equidistant time windows of length ΔT . Each EV k is characterized by $\langle t_k^a, t_k^l, CR_k, E_k \rangle$ indicating its arrival time, departure time, maximum power limit, and charging volume. This information is available once the vehicle is plugged into the system. We assume that there are sufficient number of chargers for all arrival vehicles and sufficient energy for charging. This assumption makes sense since in practice vehicles will not be allowed to enter a full parking station, and the charging lots are usually opened according to the design power capacity. The charging system creates a schedule (i.e., the charging time and the corresponding power for each vehicle) to achieve certain goals. In this study, we address two different objectives: (1) minimizing total charging cost and (2) minimizing the peak load. In practice, EVs arrive at parking lots at different times, such that the arrival time and other information of the vehicles (e.g., the charging volume and power limit) are not known in

TABLE I
PRIMARY NOTATIONS USED IN THIS ARTICLE

Notation	Description
E_k	Charging volume of vehicle k
CR_k	Maximum power limit of vehicle k
t_k^a	Arrival time of vehicle k
t_k^l	Departure time of vehicle k
$STATUS_{ji}$	1 if vehicle j is parking during time window i ; otherwise it is 0
ΔT	Length of the time window
N	Number of time windows
K	Number of vehicles
T_k	Required charging time of vehicle k
t_k^e	Charging end time of vehicle k
C_k	Cost for vehicle k
c_i	Unit electricity price in time window i
D_i	The load in time window i without accounting for current vehicle (and future vehicles)
L_i	The load in time window i accounting for current vehicle (and future vehicles)
L^*	Optimal result for the peak load
UL	Upper bound of L^*
LL	Lower bound of L^*
P_{ki}	opt. variable , Charging power available in time window i for vehicle k

advance. Thus, in essence, the problem should be addressed in a dynamic manner.

A rolling-horizon optimization framework is proposed in this study for dynamic EV charging. The research paradigm is shown in Fig. 1. The framework consists of two major components: a time window model and an optimization model. The inputs to the model include the vehicle arrival time, expected departure time, charging volume and power limit. The time window model calculates the number of time windows and numbers them according to when a vehicle arrives. Then, the information of time windows is passed to the optimization model which outputs the charging schedule for the arriving vehicle.

The rolling-horizon optimization framework is event-based, and is triggered every time a vehicle is plugged into the system. At each event, the number of time windows and their indexes are updated. For the objective of minimizing the total charging cost (Fig. 1a), the only input required is the information of current vehicle. This is enough to optimize the solution globally, as will be proven in Section III.C2). Unlike the first objective, to minimize the peak load (Fig. 1b), an input of the system load state is needed in addition to the current vehicle information. The input may also include future vehicles' information depending on whether a prediction is incorporated. Then, the system load state will be updated recursively with the charging schedule. In the following, we first introduce the uncoordinated model, followed by models for two objectives.

B. Uncoordinated Mode

To demonstrate the benefit of optimal charging schedules, the uncoordinated mode is used as the benchmark for

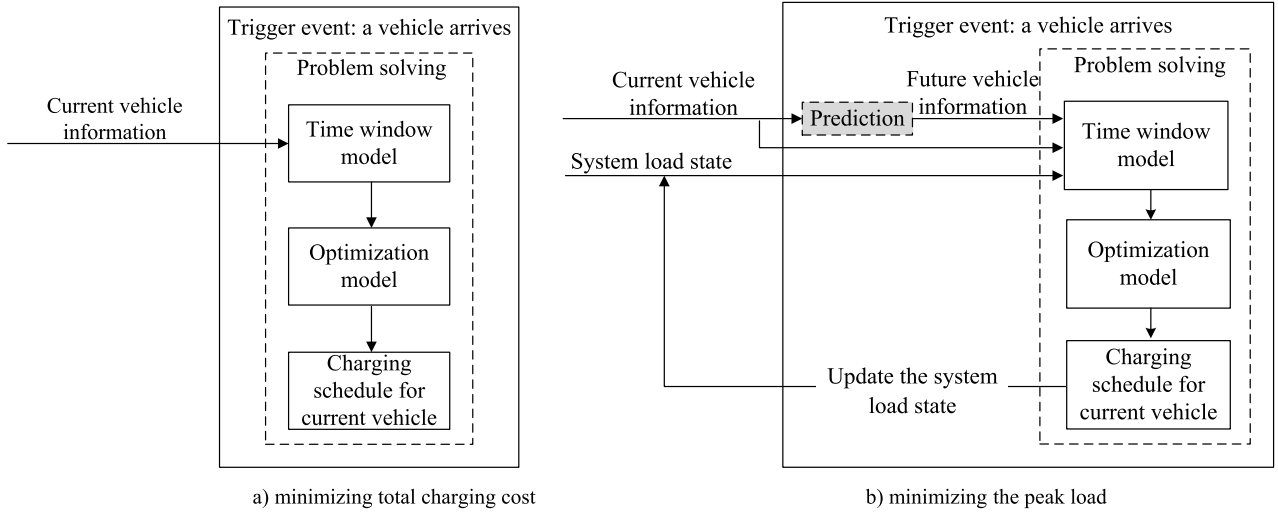


Fig. 1. Research paradigm of the models.

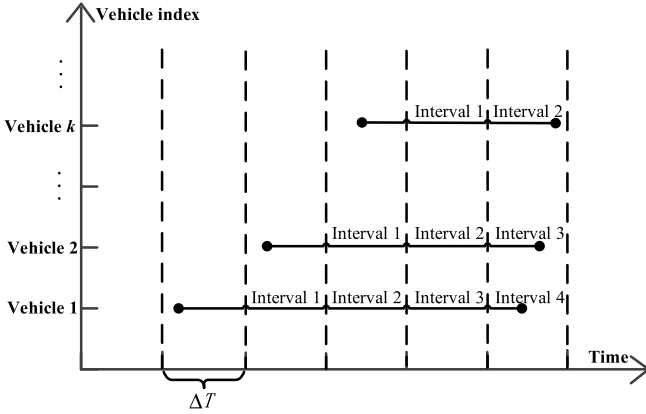


Fig. 2. Illustration of moving time windows.

comparisons, which is also commonly used in state-of-the-practice [14]. In this mode, the vehicle will be fully charged with the maximum power once plugged into the system. The actual end time depends on whether the fully charged time is larger than the due time.

The required charging time and the charging end time of vehicle k are formulated as follows:

$$T_k = \frac{E_k}{CR_k} \quad (1)$$

$$t_k^e = \min(t_k^a + T_k, t_k^l) \quad (2)$$

C. Objective 1: Minimizing the Total Charging Cost

Under Objective 1: minimizing the total charging cost, the EVs are required to charge as much as possible during low-price periods in order to save charging costs. Here, we introduce the concept of a moving time window.

As shown in Fig. 2, the time horizon is divided into a number of identical time windows of length ΔT . The charging power in an interval is kept constant. Therefore, the number of time windows within the range between the vehicle arrival

time t_k^a and departure time t_k^l is:

$$N = \lceil t_k^l / \Delta T \rceil - \lceil t_k^a / \Delta T \rceil \quad (3)$$

where $\lceil \cdot \rceil$ is the notation of the ceiling function.

Since an EV will start being charged only at the start time of a time window, additional holding time may be induced. On the other hand, a vehicle might leave before the end time of the last time window, which leads to a waste of energy. Since the charging power in an interval remains constant, more flexibility could be provided when the length of the time window is relatively short. In this study, the length of the time window (ΔT) was taken as 1 minute.

1) Model Formulation: Since the pricing and arrival time of each EV are independent, the charging schedule of the preceding vehicles would not affect that of vehicles that arrive in the future. As such, the greedy algorithm can be used to solve the problem. That is, the overall schedule can be optimized by optimizing the charging schedule for individual vehicle (see Section III.C2) for detailed proof). The formulation is given as follows:

$$\min \left(\sum_{k=1}^K C_k \right) = \sum_{k=1}^K \min(C_k) \quad (4)$$

where Eq. (4) specifies that the minimum total cost over all of the whole period equals the summation of the minimum charging cost for each vehicle. As a result, the optimization problem for vehicle k can be formulated as follows:

$$\min \sum_{i=1}^N P_{ki} \times \Delta T \times c_i \quad (5)$$

$$\text{s.t. } 0 \leq P_{ki} \leq CR_k, \quad \forall i \in [1, N] \quad (6)$$

$$E_k = \sum_{i=1}^N (P_{ki} \times \Delta T) \quad (7)$$

The objective function (5) minimizes the charging cost for vehicle k , and is defined as the sum of the product of the energy demands in each time window and the corresponding prices. Eq. (6) ensures that the charging power does not exceed the upper limit. Eq. (7) expresses that the charging volume

of vehicle k is the sum of the energy demands in each time window.

2) *Model Properties:* The purpose of this section is to prove that the minimum charging cost problem has an optimal substructure and the greedy-choice property. This indicates that a globally optimal solution can be assembled by making locally optimal greedy choices. In other words, the charge schedule that minimizes the charging cost of each individual vehicle ensures the minimization of total charging cost.

Lemma 1: The minimum charging cost problem has an optimal substructure: Let $S_{\alpha\beta}$ denote the minimum charging cost problem for vehicle α , vehicle $\alpha+1, \dots$, and vehicle β . The optimal solution is $\{\vec{P}_\alpha, \vec{P}_{\alpha+1}, \dots, \vec{P}_\gamma, \vec{P}_{\gamma+1}, \dots, \vec{P}_\beta\}$, and the corresponding objective function value is $\sum_{k=\alpha}^{\beta} C_k$. Then for the subproblems $S_{\alpha\gamma}$ and $S_{(\gamma+1)\beta}$, their optimal solutions are $\{\vec{P}_\alpha, \vec{P}_{\alpha+1}, \dots, \vec{P}_\gamma\}$ and $\{\vec{P}_{\gamma+1}, \vec{P}_{\gamma+2}, \dots, \vec{P}_\beta\}$, respectively, and the corresponding objective function values are $\sum_{k=\alpha}^{\beta} C_k$ and $\sum_{k=\gamma+1}^{\beta} C_k$, respectively.

Lemma 2: The minimum charging cost problem has a greedy-choice property: for any nonempty subproblem $S_{\alpha\beta}$, let $\{\vec{P}_\lambda\}$ denote the charging schedule of vehicle β in chronological order, then \vec{P}_λ belongs to one of the solution sets.

Proposition 1: The minimum charging cost problem has the greedy-choice property which means that a globally optimal solution can be assembled by making locally optimal greedy choices.

D. Objective 2: Minimizing the Peak Load

As discussed above, uncoordinated EV charging would increase the peak-time demand and overload the grid, which imposes higher strains on the generation units, and transmission and distribution systems. As such, another objective, which is very relevant to EV charging, is to minimize the peak load. The principle is to transfer the charging load from the peak hours to off-peak hours to achieve load valley-filling and reduce the peak demand load.

In line with Section III.C, the studied period is divided into a number of time windows with a length of ΔT . Let \vec{D} denote the system load vector across time windows, in which the value of each component is set to 0 initially. Given a newly arriving vehicle and the corresponding charging schedule \vec{P}_k , the system load state will be updated as follows.

$$\vec{D} := \vec{D} + \vec{P}_k \quad (8)$$

1) *Model Formulation:* Similar to Section III.C, we develop an optimization model for vehicle k with the objective of minimum peak load, which can be formulated as follows:

$$\min_{i \in [1, N]} \max_{i \in [1, N]} L_i \quad (9)$$

$$\text{s.t. } D_i + P_{ki} = L_i, \quad \forall i \in [1, N] \quad (10)$$

$$E_k = \sum_{i=1}^N (P_{ki} \times \Delta T) \quad (11)$$

$$0 \leq P_{ki} \leq CR_k, \quad \forall i \in [1, N] \quad (12)$$

Eq. (9) is the objective function for minimizing the peak load. Eq. (10) calculates the load of each time window.

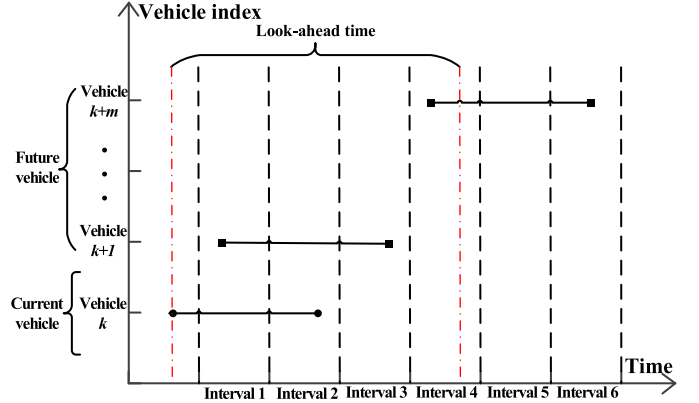


Fig. 3. Illustration of time windows and look-ahead time.

Eq. (11) specifies that the total charging volume of vehicle k equals the summation of the charging volumes of each time window. Eq. (12) ensures that the charging power P_{ki} does not exceed the power limit of vehicle k . L_i represents the load in time window i accounting for vehicle k . D_i denotes the load in time window i without accounting for vehicle k , which is also a component of the system load vector \vec{D} . P_{ki} is a component of the charging vector \vec{P}_k .

2) *Model Properties:* Proposition 2: The minimum peak load problem does not have the greedy-choice property.

E. A Non-Myopic Prediction-Based Charging Strategy for Objective 2

Proposition 2 indicates that the problem cannot be optimized globally by making greedy-choices for each vehicle. Taking Fig. 18 as an example, if the information of vehicle 2 can be known in advance or predicted, and vehicle 1 is charged with a relatively larger power as shown in Fig. 18(b) before vehicle 2 arrives, more idle power capacity could be available for later arriving vehicles. In this way, global optimality could be achieved. The commuting patterns, particularly on workdays, are quite regular and can be reproduced to a certain extent. This opens up more opportunities for optimal charging via prediction. Motivated by this observation, we propose a non-myopic charging strategy, which accounts for anticipated future requests, to achieve a globally optimal solution with Objective 2.

To illustrate the prediction-based strategy, as shown in Fig. 3, once vehicle k arrives, the system will first predict the relevant information for future vehicles $k+1, k+2, \dots, k+m$ within the look-ahead time, such as the arrival time, charging volume and power limits. Subsequently, the charging schedule for vehicle k will be made accounting for the predicted information of future vehicles.

The time windows are numbered from the arrival time of current vehicle k to the departure time of all vehicles predicted to arrive within the look-ahead time. At the instant when vehicle k arrives, the number of time windows is given as follows:

$$N = \lceil \max(t_k^l, t_{k+1}^l, \dots, t_{k+m}^l) / \Delta T \rceil - \lceil t_k^a / \Delta T \rceil \quad (13)$$

To track the parking state of each vehicle, we introduce a new variable $STATUS_{ji}$ to indicate whether vehicle j ($j \in [k, k+m]$) is parking during time window i ($i \in [1, N]$). If the vehicle is parking, $STATUS_{ji} = 1$; otherwise, $STATUS_{ji} = 0$. For example, if vehicle k is parking in interval 2, then $STATUS_{k2} = 1$; if vehicle $k+m$ is not parking in interval 2, then $STATUS_{(k+m)2} = 0$.

Naturally, when the look-ahead time is long, more future vehicles can be included, and the outcome will be closer to the globally optimal solution. However, a longer look-ahead time increases the computational burden. Therefore, it is necessary to find the optimal look-ahead time by balancing the algorithm effectiveness and efficiency.

1) Model Formulation: For a newly arriving vehicle k and the corresponding m vehicles within the look-ahead time, the minimum peak load problem can be formulated as follows:

$$\min \max_{i \in [1, N]} L_i \quad (14)$$

$$\text{s.t. } D_i + \sum_{j=k}^{k+m} P_{ji} = L_i, \quad \forall i \in [1, N] \quad (15)$$

$$E_j = \sum_{i=1}^N (P_{ji} \times \Delta T), \quad \forall j \in [k, k+m] \quad (16)$$

$$\begin{cases} 0 \leq P_{ji} \leq CR_j, & \text{if } STATUS_{ji} = 1 \\ P_{ji} = 0, & \text{if } STATUS_{ji} = 0 \end{cases} \quad \forall i \in [1, N], \quad \forall j \in [k, k+m] \quad (17)$$

Eq. (14) is the objective function that minimizes the peak load. Eq. (15) calculates the load of each time window. Eq. (16) specifies that the total charging volume of each vehicle $j \in [k, k+m]$ equals the summation of the charging volume in each time window. Eq. (17) ensures that if vehicle j is parking in time window i , the decision variable P_{ji} should not exceed the power limit of vehicle k ; otherwise, it is 0. L_i represents the load in time window i accounting for vehicles $k \sim k+m$. D_i denotes the load in time window i without accounting for vehicles $k \sim k+m$.

2) Solution Method: To solve this conundrum, we propose a heuristic algorithm that combines multi-commodity network flow model with a customized bisection search in a rolling horizon framework. The heuristic algorithm can be divided into two processes: (a) determination of system's optimal load and (b) assignment of the charging power P_{ji} to different time windows. In this heuristic algorithm, L and P_{ji} are decision variables, where $L := L_i$ is the objective function in maximum flow problem and the decision variable in the bisection search algorithm. Let us consider L^* be the optimal result for the peak load, then there are two possible outcomes. When $L < L^*$, then the charging demand of at least one vehicle cannot be satisfied; when $L > L^*$, L is not an optional solution, although it satisfies the constraints. Hence, we adopt a bisection search algorithm to determine the optimal load L^* within the upper limit UL and lower limit LL . Given the load L , the charging events across time windows can be represented by the multi-commodity network flow model. The question is how to distribute the charging power P_{ji} while satisfying the charging demands.

a) Representation of network flow: The problem can be abstracted as a maximum flow problem, which involves finding

a maximum flow through a single-source, single-sink flow network. The objective is to determine the charging power P_{ji} given a predefined system load L , while satisfying the charging demands. For a newly arriving vehicle k and the future predicted vehicles $k+1, k+2, \dots, k+m$, the following notations are used to represent the flow network $G = (V, A)$:

- The set of nodes V consists of (i) the origin of the network, O , (ii) the destination of the network, D , (iii) the vehicle nodes $k, k+1, k+2, \dots, k+m$, with $m+1$ nodes in total, (iv) the time window nodes $1, 2, 3, \dots, N$, with N nodes in total.
- The set of edges A consists of (i) the edges between the origin of network, O , and the vehicle nodes, which is $m+1$ edges in total, (ii) the edges between the vehicle nodes and the time window nodes, with no more than $N(m+1)$ edges in total, (iii) the edges between the time window nodes and the destination of network D , with N edges in total.

Fig. 4 shows the problem representation characterized by the network flow model. The value on each link represents the flow capacity. The number of links originating from the origin equals the number of vehicles, and the link flow E_k represents the charging volume required by vehicle k . The time window nodes connected by vehicle k represent the corresponding charging time. The charging volume in each time window should not exceed the product of the maximum power limit and length of the time window. The link capacity from a time window node to the destination node specifies that in this time window, the total charging volume should not exceed a critical value, which equals the product of the time window length ΔT and the deviation between the maximum load and the current system load $L - D_i$.

Obviously, the maximum flow will not exceed $\sum_{j=k}^{k+m} E_j$. If the network maximum flow is equal to $\sum_{j=k}^{k+m} E_j$, then the charging demand is satisfied. On the other hand, if the maximum flow is less than $\sum_{j=k}^{k+m} E_j$, then there is unmet charging demand. Typically, there is no closed-form solution for the exact L^* value. We can use the following bisection search approach to find an approximation of L^* , which can be arbitrarily close to the true optimal value.

b) Bisection search: Given the upper and lower bound UL and LL , we can use the following bisection method in Algorithm 1 to find the optimal load L^* . More specifically, develop a network flow model $G = (V, A)$ given $L = (UL + LL)/2$, and solve it using typical maximum flow algorithm, such as the Ford-Fulkerson algorithm. If the charging demand is satisfied, then $UL = L$; otherwise, $LL = L$. Through a number of iterations, there will exist an approximation of L close to L^* within a certain accuracy threshold. Based on this, the charging schedule for vehicle k can be obtained.

c) Upper bound and lower bound of L^ :* In this section, we derive the upper bound and lower bound on the peak load. We rely on these bounds in the bisection search algorithm to restrict the solution space. When the optimal load peak L^* is found, the charging demand is satisfied exactly with a maximum flow of $\sum_{j=k}^{k+m} E_j$. In Fig. 4, the destination and

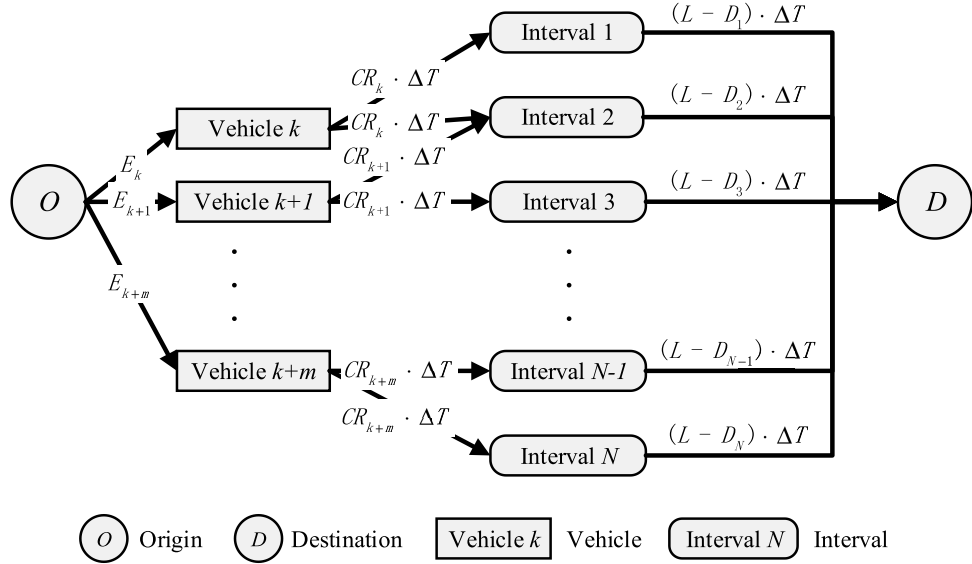


Fig. 4. Representation of the network flow model.

Algorithm 1 The Bisection Method to Approximate L^*

INPUT: upper limits UL , lower limits LL , accuracy threshold
1: while $UL - LL <$ accuracy threshold
2: $L := (UL + LL)/2$;
3: Develop a network flow model $G = (V, A)$ given L , and solve it using typical maximum flow algorithm, such as the Ford-Fulkerson algorithm;
4: if the charging demand is satisfied then
5: $UL = L$;
6: else
7: $LL = L$;
8: end if
9: end while
RETURN: charging schedule for vehicle k

other nodes apart from the destination can be treated as a cut set with a capacity of $(N \cdot L^* - \sum_{i=1}^N D_i) \cdot \Delta T$. According to the max-flow min-cut theorem, the volume of any feasible flow should not exceed the capacity of any cut set. This is equivalent to the relaxation of constraints, see detailed proof in Proposition 4. Therefore, we have the following inequalities:

$$(N \cdot L^* - \sum_{i=1}^N D_i) \cdot \Delta T \geq \sum_{j=k}^{k+m} E_j \quad (18)$$

To avoid the nonnegative link, the optimal peak load L^* should not be less than the system load D_i in each time window.

$$L^* \geq D_i, \quad \forall i \in [1, N] \quad (19)$$

To further reduce the computational complexity, the lower bound can be the greater of Eqs. (18) and (19), that is,

$$LL = \max \left(\left(\sum_{j=k}^{k+m} E_j / \Delta T + \sum_{i=1}^N D_i \right) / N, \max_{i \in [1, N]} D_i \right) \quad (20)$$

For the minimization problem, the upper bound corresponds to the value of objective function given any feasible solution satisfying the constraints. If all vehicles start being charged at the arrival time with “minimum power” so that they are fully charged immediately before the departure time, then the charging power of vehicle j is:

$$\begin{cases} P_{ji} = \frac{E_j}{t_j^a - t_j^l}, & \text{if } STATUS_{ji} = 1 \\ P_{ji} = 0, & \text{if } STATUS_{ji} = 0 \end{cases} \quad \forall i \in [1, N], \quad \forall j \in [k, k+m] \quad (21)$$

Evidently, such a solution satisfies all constraints. Substituting Eq. (21) into Eq. (15) yields the upper bound of the objective function as follows:

$$UL = \max_{i \in [1, N]} (D_i + \sum_{j=k}^{k+m} P_{ji}) \quad (22)$$

3) *Model Properties:* In the previous sections, we have shown that the prediction-based charging strategy can be abstracted as a network flow model that can be solved by the maximum flow and the bisection search method. We now investigate the complexity of the heuristic algorithm.

Proposition 3: Assume that the number of bisection searches is f times, such a prediction-based charging strategy can be solved in polynomial time with complexity of $O(VA^2f)$.

Proposition 4: For the peak load minimization problem, the lower bound is the results under the relaxation of constraints $D_i + \sum_{j=k}^{k+m} P_{ji} \leq L, \forall i \in [1, N]$.

4) *Prediction of Vehicle Information:* For the prediction-based charging strategy, the information of future arriving vehicles within the look-ahead time should be provided. The charging station can have full knowledge of future demand. This can be realized for instance, by requiring that EV owners book a parking lot along with their arrival time and charging demand through parking reservation systems [16], [25], [26]. Before the parking reservation

systems are fully enforced, the charging station may also gain partial knowledge on future demand by prediction [6]. In practice, the commuting patterns, particularly on workdays, are quite regular and can be estimated to a certain extent. Thus, the statistics of EV arrival process often exhibit periodicity. For example, the arrival rate of residential EV charging demand could have a periodicity where the period is one day. Given this fact, the vehicle state information can be estimated based on historical data.

In this section, we propose a potential prediction approach for future arriving vehicles based on historic data (though being not the research focus of this paper). In principle, it can be substituted by any other methods or empirical rules, which would not affect the generalization of the framework. A prediction is triggered each time a vehicle arrives. In this study, the kernel density estimation model is adopted to establish a curve representing the historic accumulative vehicle arrivals versus arrival time. With the fitted curve, the arrival time and the number of future vehicle m within a rolling horizon can be estimated. This is done by moving horizontally on the diagram for each arriving vehicle until intersecting the cumulative curve and then vertically; this results in the predicted arrival time. Other various machine learning-based algorithms in the literature can also be adopted to predict vehicle arrival time, which is out of the scope of this study. We now discuss the prediction of other vehicle state information (i.e., the parking time, charging volume, and power limit), given that the predicted future vehicle arrival time.

Since the charging volume and parking time are continuous variables, it is reasonable to take the average of the historical data as the predicted values. In contrast, the charging power limit is a discrete variable. According to the principle of maximum likelihood, it is more reasonable to take the mode of the historical data as an estimate, where the mode represents the value that is repeated most often in the dataset. Given the arrival time t_k^a for vehicle k and the corresponding look-ahead time, the solution framework for prediction is provided in Algorithm 2. The validation of prediction accuracy will be provided in Section IV.E.

IV. SIMULATION EXAMPLE

A. Case Description

The study case is the Citic Plaza, a multi-story car park in Guangzhou, with a total of 900 parking spaces. The historical vehicle arrival information is utilized to mimic the workplace charging, and it is found that the arrival time of commuting vehicles follows a normal distribution $N(9, 0.5^2)$ with a mean of 9 (h) and a standard deviation of 0.5 (h), while the arrival time of other vehicles follows a uniform distribution $U(0, 24)$. In addition, the parking time for overall vehicles follows a normal distribution $N(8, 0.5^2)$ with a mean of 8 (h) and a standard deviation of 0.5 (h). The corresponding number of parking spaces is assumed to be the maximum number of charging lots.

Fig. 5 shows the commercial time-of-use electricity price for the parking lot. The price is the lowest from 24:00 to 08:00, while it is the highest in the period of 14:00 to

Algorithm 2 Solution Framework for Predicting State Information of Future Arriving Vehicles

INPUT: vehicle information $(t_k^a, t_k^l, E_k, CR_k)$

1: Obtain the arrival time for m vehicles during the look-ahead time, $t_{k+1}^a, t_{k+2}^a, \dots, t_{k+m}^a$.

2: For the predicted vehicle j ($j \in [k + 1, k + m]$) arriving at time t_j^a , estimate the charging volume, parking time, and charging power limit using historical data within a duration of 15 minutes. More specifically, take the average of charging volume and parking time, and the mode of the charging power limit of vehicles arriving from $\lfloor t_j^a/15 \rfloor \times 15$ to $(\lfloor t_j^a/15 \rfloor + 1) \times 15$ as the estimate.

3: Repeat the above processes until the prediction for m vehicles is completed.

RETURN: prediction for m vehicles, arriving within the look-ahead time, of $(CR_j, E_j, t_j^a, t_j^l (j \in [k + 1, k + m]))$

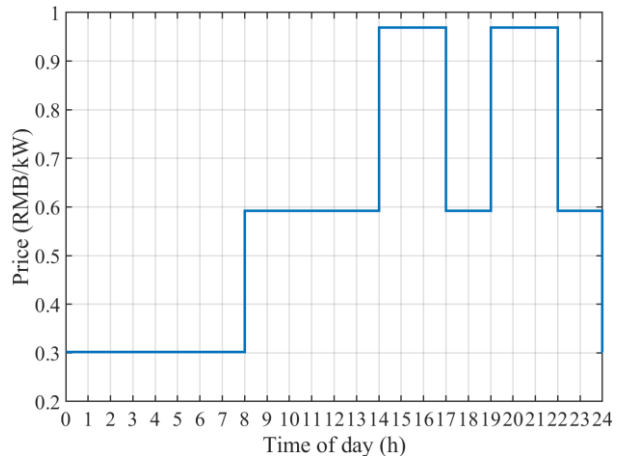


Fig. 5. Time of use charging price.

17:00 and 19:00 to 22:00. Generally, an EV consumes 15 to 20 kw per 100 kilometers. According to our survey, the average daily travel distance in Guangzhou is 36-40 kilometers. Then, the minimum and maximum power consumption can be calculated as $36 \times 15/100 = 5.4$ kW and $40 \times 20/100 = 8$ kW, respectively. Therefore, the required charging volume is approximated as a uniform distribution $U(5.4, 8)$. Since there are a total of 900 parking spaces in the Citic Plaza, the numbers of arriving vehicles are taken as 900, 600, 300 under high, moderate, and low demand circumstances, respectively.

B. Optimization of Look-Ahead Time

The look-ahead time, during which a number of future charging requests are taken into account, is a new feature in the prediction-based coordinated charging strategy (Section III, E). In this section, we analyze the impact of the length of the look-ahead time on system performance. Generally, a longer look-ahead time indicates that the charging decision is made coordinately with more information of historical vehicles is utilized for prediction, which may improve the prediction

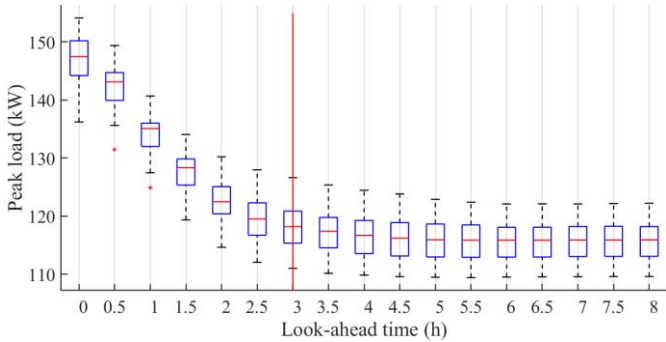


Fig. 6. The peak load under different look-ahead times.

accuracy. However, a longer look-ahead time will also increase the computational burden. Therefore, it is imperative to optimize the look-ahead time by balancing the algorithm's effectiveness and efficiency.

To illustrate, let us consider a case where the peak arrival ratio is 50%, and the demand level is low. The peak arrival ratio is defined as the ratio of the number of commuting vehicles (numerator) to the total number of vehicles (denominator). Generally, a higher peak arrival ratio indicates a more regular commuting pattern. The myopic charging strategy without prediction can be regarded as a special case of a non-myopic strategy without any look-ahead time. We generated 30-day datasets according to the aforementioned distributions. Fig. 6 shows the peak load under different look-ahead times using a box and whisker plot. The peak load decreases in an exponential manner with increases in the look-ahead time. This indicates that an increase in the number of anticipated arriving vehicles contributes to reducing the peak load. However, there is a cut-off point (3 h in this case) beyond which the reduction of peak load becomes trivial. In other words, there is a non-effect region for prediction. Therefore, to ensure algorithm effectiveness and efficiency, the optimal look-ahead time can be set as 3 h.

We further investigate the optimal look-ahead time under various combinations of peak arrival ratios and demand levels, and the results are shown in Fig. 7. The vertical lines in the figures represent the optimal look-ahead time. As we can see, the optimal look-ahead time decreases as the peak arrival ratio increases. This is because a higher peak arrival ratio indicates a more concentrated arrival time distribution for commuting vehicles and a weakened influence of vehicles arriving during off-peak hours, such that the system performance will rely more on the vehicles arriving in peak hours. As a result, a shorter look-ahead time is required to forecast the vehicle arrivals when the peak arrival ratio is higher. We also observe that the optimal look-ahead time is longer when the demand level is higher. One potential reason is that with a higher demand, the effect of future arriving vehicles becomes more significant. Consequently, more predicted vehicles (and thus longer look-ahead time) are needed to achieve a better performance.

C. Computation Performance of the Proposed Algorithm

In this section, we analyze the computational efficiency of the proposed algorithm. The search times of the bisection

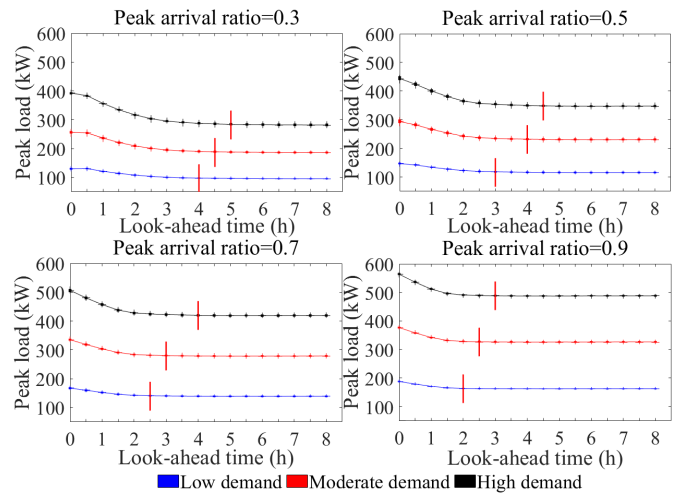


Fig. 7. The peak load under different look-ahead time, peak arrival ratios, and demand levels.

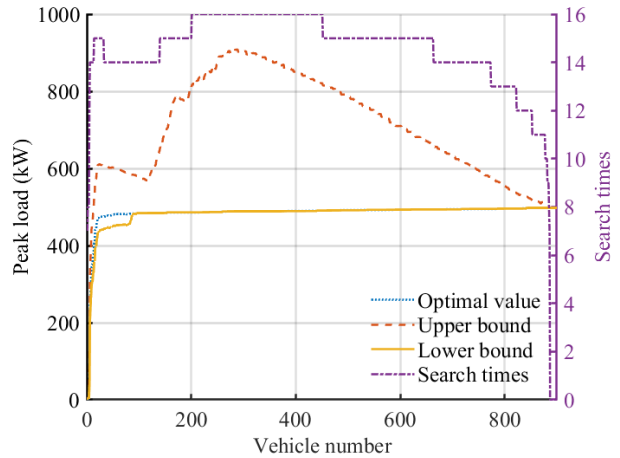
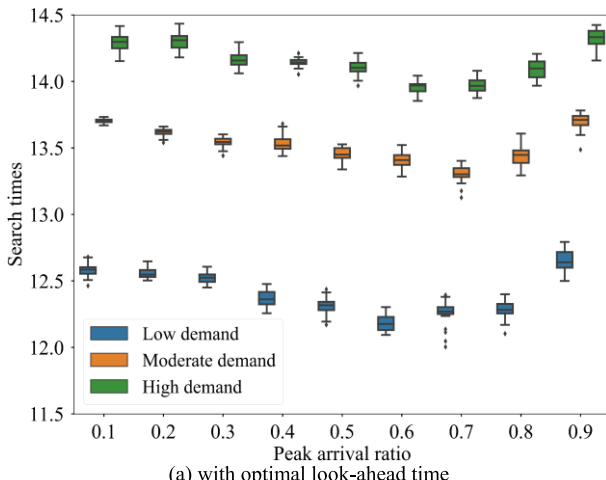


Fig. 8. The performance of the algorithm with dynamic arriving vehicles.

search algorithm is determined by the initial upper and lower bounds. To reduce the accumulated errors while improving the computation efficiency, in this study the convergence threshold is set as 0.01 kW.

Fig. 8 shows the change of initial upper bound, lower bound and the corresponding optimal value, as well as the search times with dynamic arriving vehicles over time, where the demand is high and the peak arrival ratio is 90%. As we can see, the optimal value is closer to the lower bound, and the optimal value begins to be identical to the lower bound after 100-th vehicle arrives, which corresponds to the rush hour when the peak load happens. With the increase of arriving vehicles, the search times (the number of iterations) first increases before hitting the threshold, followed by a long plateau, and then decreases drastically to 0. This is because the heavy charging demand during the peak hours enlarges the difference between the upper bound and lower bound, which leads to more search times. During the off-peak hours, the (historic) peak load remains the same, and the gap between the upper bound and lower bound narrows down, which leads to the reduction of search times. The search times drops



(a) with optimal look-ahead time

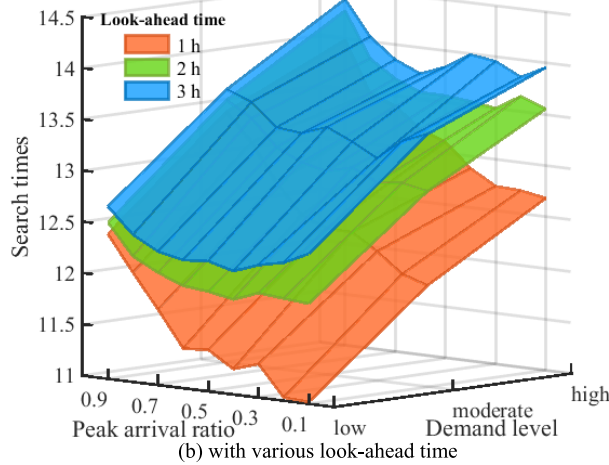


Fig. 9. Search times under various demand levels and peak arrival ratios.

to 0 immediately after the last vehicle arrives. Overall, the computational efficiency is quite good, with an average search times of 14.

We analyze the algorithm performance under different traffic conditions using the 30-day datasets. Fig. 9(a) shows the search times under various demand levels and peak arrival ratios using a box and whisker plot, given the optimal look-ahead time. One can see that the algorithm requires a larger number of iterations to reach the optimal solution as the demand level increases, which is expected since higher charging demand enlarges the difference between the upper bound and lower bound. On the other hand, the search times changes slightly with the increase of peak arrival ratio. This indicates that peak arrival ratio has little influence on the difference between the upper bound and lower bound.

Fig. 9(b) presents the search times under various demand levels and peak arrival ratios with various look-ahead time. We observe that the search times increases with the increase of look-ahead time, which is due to the increasing number of variables (vehicles) that are added to the calculation at each iteration. In addition, when the peak arrival ratio is higher, the impact of look-ahead time on the search times becomes less significant. This is because the number of

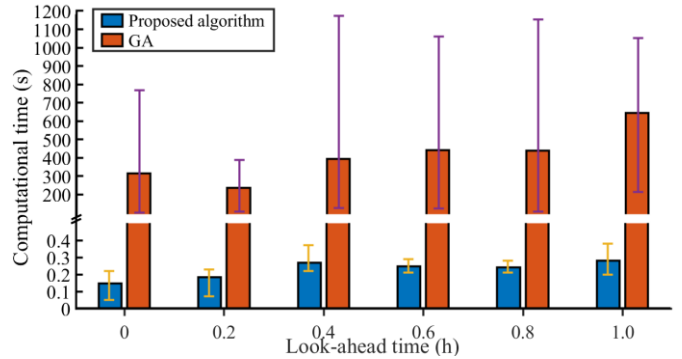


Fig. 10. Comparison of computational time.

vehicles involved in calculation is already large under high peak arrival ratio, such that any increase of look-ahead time contributes less to the search times.

In the literature, a variety of intelligent algorithms have been proposed to deal with EV charge scheduling problems [5]. To validate the advantage of algorithmic computation efficiency, it is imperative to compare the computational time of our proposed algorithm with those of the state-of-the-art algorithms. To be representative, we select the genetic algorithm (GA) as the benchmark, which is a typical type of intelligent algorithms with random search. The programs are implemented in Matlab 2018b on an Intel(R) Core(TM) i5-5200U CPU @ 2.20 GHz with 8.0GB DDR3. To illustrate, let us consider a case where the peak arrival ratio is 10%, and the demand level is low. Fig. 10 shows the average CPU time for five instances (the first five arriving vehicles) under different look-ahead time. As we can see, the solution time of GA is significantly higher than that of our algorithm, and the gap becomes larger when the look-ahead time increases. More specifically, the solution time of our algorithm only needs less than 0.5 second in all scenarios, whereas that of GA increases rapidly as the look-ahead time increases, and consumes approximately 10 min with only a prediction horizon of one hour. This suggests that the proposed algorithm can be efficiently applicable for online charge scheduling. On the contrary, GA cannot be used for online scheduling since it is nearly impossible to obtain the optimal results in a reasonable time, particularly when the demand is heavy and the look-ahead time is long. Better still, from the error bars we observed that the stability of our algorithm is much stronger than that of GA.

D. Model Comparisons

In this section, we compare the system performance for different charging strategies. Our optimization models can be retrofitted to include multiple objectives by using a lexicographic method. The principle is that after the first objective is optimized, the result is added to the model of the second objective as a constraint in the second stage. This ensures that the total cost is not worse than the result of the first stage. Since the peak load minimization is associated with the power capacity design, here the first objective is to minimize

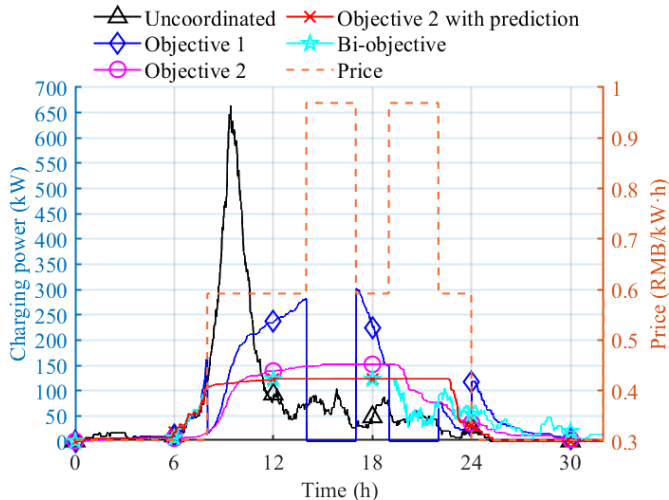


Fig. 11. The charging power profile under different strategies.

TABLE II
SYSTEM PERFORMANCE UNDER DIFFERENT STRATEGIES

Performance	Uncoordinated	Objective 1	Objective 2	Objective 2 with prediction	Bi-objective
Peak load power (kW)	663.90	301.76	152.10	123.14	123.10
Total charging cost (RMB)	1261.02	1089.70	1445.79	1424.36	1307.24
Average charging cost (RMB/veh)	4.20	3.63	4.82	4.75	4.36

the peak load while the second objective is to minimize the charging cost. Taking the base case as an example (peak arrival ratio of 50% and a low demand level), we conduct simulations for the following models: Uncoordinated, Objective 1, Objective 2 without prediction, Objective 2 with prediction (under optimal look-ahead time), and Bi-objective. The system load and charging cost are selected as the evaluation indicators.

Fig. 11 shows the aggregated charging power under different strategies. As presented, the charging power first increases and then drops during the period from 08:00-10:00 under the uncoordinated strategy. The charging power is distributed in the low-price period under Objective 1. In comparison, the peak load is the lowest and appears as a smooth hump under Objective 2 with prediction. In particular, compared to Objective 2 without prediction, the charging power reaches its peak earlier and is spread over a wider range. This is because with prediction, the system is able to charge the vehicles with a relatively larger power in advance, which reduces the future peak load. Under the bi-objective strategy, the peak load is identical to that of Objective 2 with prediction, while the charging power during evening peak spreads over a wider range of low tariff period.

Solving the optimization problems for the collected datasets under the different strategies yields the system performance shown in Table II compared to the uncoordinated strategy, the peak load and charging cost are considerably lower under Objective 1. The total cost savings for 300 vehicles is 171.32 RMB with an average savings rate of 13.57%.

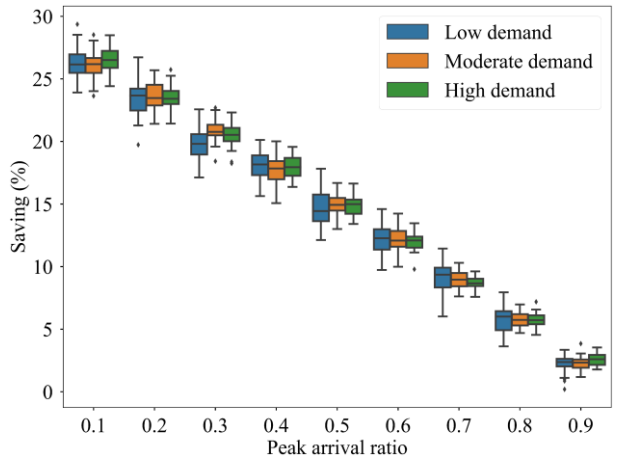


Fig. 12. Charging cost savings under Objective 1 relative to the uncoordinated strategy.

The peak load reductions under Objective 2 with and without prediction are 81.45% and 77.09%, respectively, at the expense of an increase in charging costs of 14.65% (0.62 RMB per vehicle) and 12.95% (0.55 RMB per vehicle), respectively. Compared with Objective 1, the peak load reductions under Objective 2 with and without prediction are 59.19% and 49.6%, respectively. Compared to Objective 2 with prediction, the total charging cost under bi-objective strategy is reduced by 8.22% (0.39 RMB per vehicle), while maintaining the same peak load.

To further verify the effectiveness of the models, a sensitivity analysis is conducted under various demand levels and peak arrival ratios. Again, the 30-day datasets are used for each experiment. Fig. 12 shows the cost savings under Objective 1 relative to the uncoordinated strategy. One can see that the cost savings decrease with the increases in the peak arrival ratio. This is because a number of vehicles arriving during peak hours would still be charged during the high-price period due to their expected departure time, such that the cost savings during off-peak hours is larger than that during peak hours. As a result, less cost savings can be expected when the peak arrival ratio is higher.

Fig. 13(a) presents the peak load savings by Objective 2 with prediction relative to the uncoordinated strategy. As we can see, the savings increase with the increase in peak arrival ratio at a decreasing rate. When the peak arrival ratio reaches 0.4, the improvements become trivial. This is because as vehicle arrivals become denser, the system will assign more vehicles to charge during off-peak hours, which contributes to load leveling. However, due to parking and departure time constraints, load leveling could become more difficult with an increase of the peak arrival ratio.

Fig. 13(b) presents the peak load savings under Objective 2 with prediction. The prediction could lead to load reduction of 13.4%-28.8%. The savings are reduced as the peak arrival ratio increases, and the savings increase as the demand level increases. As concluded in Section IV.B, a higher peak arrival ratio contributes to reducing the optimal look-ahead time, while a higher demand level leads to a longer optimal look-ahead time. In other words, when the peak arrival ratio

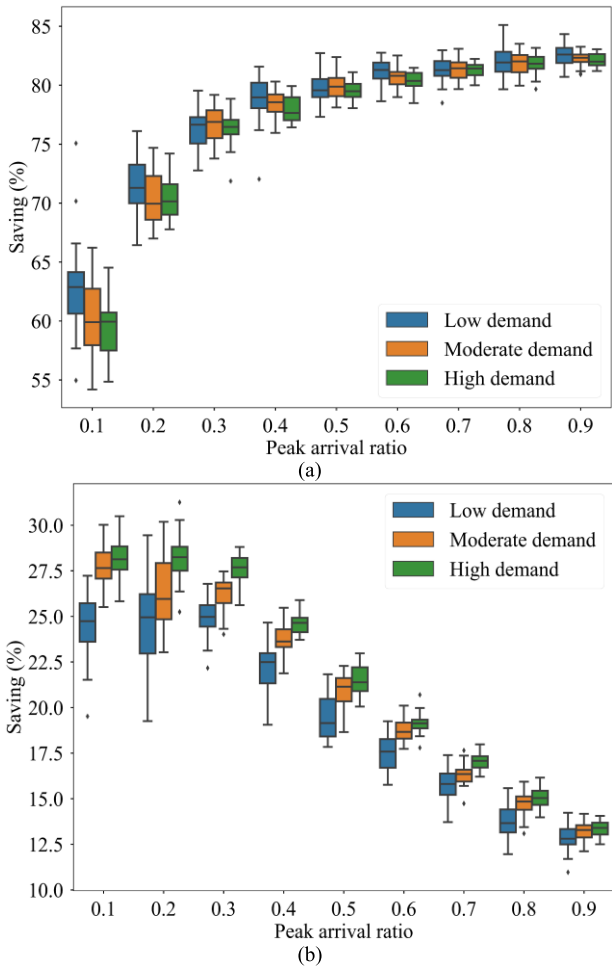


Fig. 13. Peak load savings under Objective 2 with prediction relative to (a) the uncoordinated strategy; (b) Objective 2 without prediction.

is higher and the demand level is lower, the effect of the look-ahead time is weakened such that the performance difference of strategies with and without prediction will decrease.

Moreover, we observe from Fig. 12 and Fig. 13(a) that the impact of demand levels is insignificant, particularly at high demand levels. For Objective 1, minimizing the total charging cost is effectively equivalent to minimizing the charging cost for each vehicle individually (Proposition 1). Since the cost savings for each vehicle is independent of the demand level, the impact of the demand level on the total cost savings would be limited. In contrast, the charging demand can be coordinated under Objective 2 with prediction, which mitigates the effect of the demand level to a large extent.

In addition, according to the error bars in Fig. 12 and Fig. 13, the savings variability generally decreases with increases in the peak arrival ratio or the demand level. This is because the vehicle arrival is a stochastic event; when the demand level is higher, the saving would be closer to an expected value. On the other hand, the commuting vehicles will account for a larger proportion as the peak arrival ratio increases. Since the arrival pattern of commuting vehicles is more regular and predictable, a lower variability of savings can be expected.

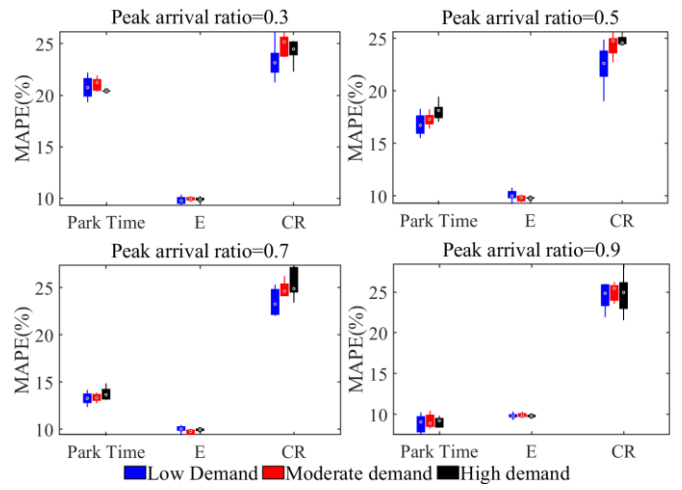


Fig. 14. Prediction performance of Algorithm 1 for parking time, power limit and charge volume.

E. Stability Analysis of the Prediction-Based Strategy

While it is shown that the non-myopic charging strategy with prediction could reduce the peak load, it is not uncommon for an operator to face prediction uncertainties in practice. Thus, it is imperative to verify the stability of such a strategy under various scenarios. In this section, using the prediction method proposed in Section III.E4) (Algorithm 2) and a cross-validation method, the impact of the prediction error on the system performance is explored under different peak arrival ratios and demand levels. To this end, the entire 30-day data are divided into training data (80%, 1st-24th day) and testing samples (20%, 25th-30th day).

Fig. 14 shows the prediction performance of Algorithm 2 for parking time, power limit (CR) and charge volume (E) under different scenarios. As we can see, the mean absolute percentage errors (MAPEs) of power limit and charge volume do not vary across different scenarios, whereas that of parking time is reduced as the peak arrival ratio increases. This is because the commuting demand is in the majority during rush hours, such that the parking time is quite regular.

As an illustration, let us consider a case where the peak arrival ratio is 50% and under low demand. The vehicle state information of the 25th day is forecasted using the historical data (1st-24th day). With the predicted information, the charging schedule and the corresponding power profile are generated. The results are compared with those of without prediction and perfect prediction. As shown in Fig. 15, the profile under prediction-based strategy reveals oscillation at approximately 10:00 am. The peak load with prediction error is higher than that with perfect prediction but lower than that without prediction, with a relative error of 12.8%.

We further analyze how the traffic conditions (i.e., demand level and peak arrival ratio) will affect the accuracy (the gap of peak load between that with perfect prediction and prediction error). The look-ahead time is set as varying from 0.25 times to 1 times of the optimal look-ahead time. Fig. 16 presents the MAPEs using a box and whisker plot. As we can see, under the same demand level and look-ahead time, the relative errors decrease as the peak arrival ratio increases. The possible

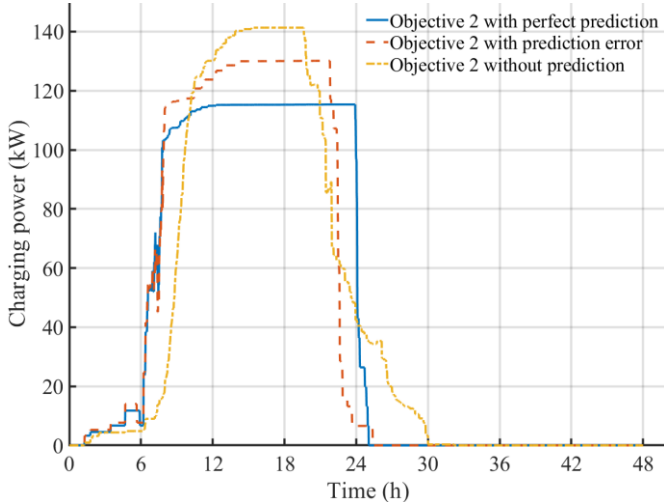


Fig. 15. System load profile under Objective 2.

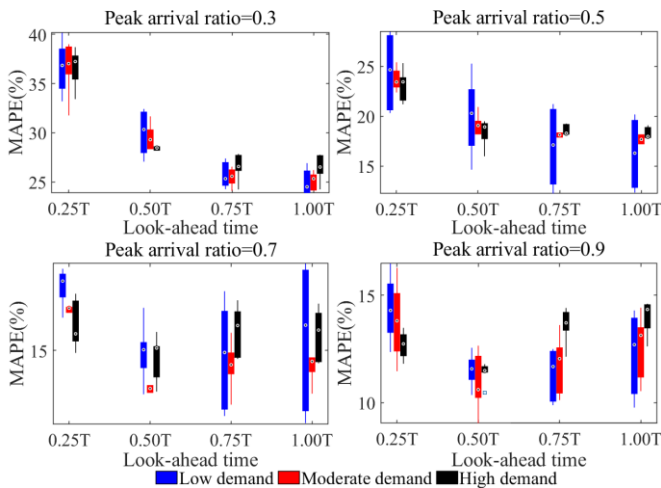


Fig. 16. Distributions of relative errors under different look-ahead time and traffic conditions.

reason is that the arrival pattern of commuting vehicles arriving in peak hours is more regular, such that more accurate prediction could be achieved. In particular, when the peak arrival ratio is larger than 0.7, the accuracy could be quite acceptable with a relative error as low as approximately 10%. This reveals promising application potentials for workplace charging where peak arrival ratio is usually high due to the characteristic of commuting demand.

V. CONCLUDING REMARKS

Efficient charge scheduling management is crucial for profitability and mass adoption of EVs. How to charge EVs in a cost-effective manner and how to mitigate overloading are two critical and open issues in the realm of EV charge scheduling. This paper investigates the model properties and efficient algorithms for the two objectives. For Objective 1, we demonstrate that the greedy-choice property applies in that a globally optimal solution can be assembled by making locally optimal greedy choices, whereas it does not apply to Objective 2. To solve to global optimality for Objective 2, we proposed a prediction-based charging strategy which

accounts for anticipated future demand within a look-ahead time. This is addressed by a heuristic algorithm combining a multi-commodity network flow model with bisection search algorithm in a rolling horizon framework. In particular, to expedite the solution speed of the bisection search algorithm, the upper bound and lower bound are derived based on the relationship between charging volume and parking time.

The proposed strategies were tested and compared under different operational settings by simulations. The impact of demand levels and peak arrival ratios on the system performance were investigated. The results showed that under the prediction-based strategy, the peak load can converge to global optimality within the effective look-ahead time. The prediction could lead to load reduction of 13.4%-28.8%. In particular, there exists an optimal look-ahead time beyond which any predicted information has little effect. The optimal look-ahead time decreases when the peak arrival ratio is higher or when the demand level is lower. The proposed algorithm is much more efficient than the state-of-the-art algorithms, and robust to the variations of demand and peak arrival ratios. We also conducted sensitivity analysis to explore the relative savings in charging cost and peak load by the proposed strategies under different peak arrival ratios and demand levels. In addition, we also proved experimentally through cross-validation that the prediction-based strategy is robust particularly under a high peak arrival ratio. This suggest a promising application potential for workplace charging, which is gaining increasing attention with the capability of overcoming the range-anxiety problem and other drawbacks of EVs [27].

This paper opens up new research directions. For example, future research may continue to incorporate an extended list of constraints under various operational settings. In addition, it would be interesting to refine the prediction approach to further improve the robustness of the prediction-based charging strategy.

APPENDIX A PROOF OF LEMMA 1

According to the principle of “cut-and-paste”: As a component of optimal solution for the master problem, the solution of each subproblem is optimal. This can be established by proof by contradiction. Assume that there is a solution set $\{\vec{P}'_a, \vec{P}'_{a+1}, \dots, \vec{P}'_\gamma\}$ that satisfies $\sum_{k=a}^\gamma C'_k < \sum_{k=a}^\gamma C_k$, then a solution set $\{\vec{P}'_a, \vec{P}'_{a+1}, \dots, \vec{P}'_\gamma, \vec{P}_{\gamma+1}, \vec{P}_{\gamma+2}, \dots, \vec{P}_\beta\}$ can be constructed that satisfies the constraints for S_{ab} . The objective function value for such a solution set is $\sum_{k=a}^\gamma C'_k + \sum_{k=\gamma+1}^\beta C_k$, which is less than the optimal value of S_{ab} , i.e., $\sum_{k=a}^\gamma C_k$. This contradicts the assumption that $\{\vec{P}_a, \vec{P}_{a+1}, \dots, \vec{P}_\gamma, \vec{P}_{\gamma+1}, \vec{P}_{\gamma+2}, \dots, \vec{P}_\beta\}$ is the optimal solution. Therefore, for the subproblem S_{ay} , the optimal solution and the corresponding objective function value are $\{\vec{P}_a, \vec{P}_{a+1}, \dots, \vec{P}_y\}$ and $\sum_{k=a}^y C_k$, respectively. Similarly, it can be proven that for the subproblem $S_{(\gamma+1)\beta}$, the optimal solution and the corresponding objective function value are $\{\vec{P}_{\gamma+1}, \vec{P}_{\gamma+2}, \dots, \vec{P}_\beta\}$, and $\sum_{k=\gamma+1}^\beta C_k$, respectively.

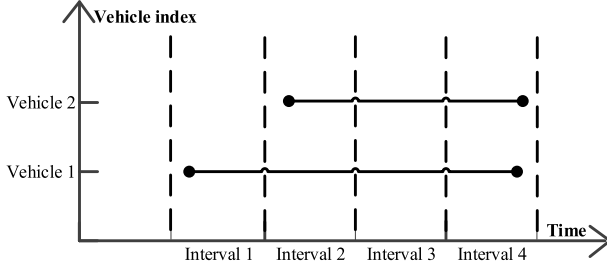


Fig. 17. Arrival time and departure time.

APPENDIX B PROOF OF LEMMA 2

Let $\{\vec{P}_\alpha, \vec{P}_{\alpha+1}, \dots, \vec{P}_\beta\}$ denote one of the optimal solution sets of $S_{\alpha\beta}$, of which $\{\vec{P}_\beta\}$ is the charging schedule of vehicle β in chronological order. If $\{\vec{P}_\beta\} = \{\vec{P}_\lambda\}$, then \vec{P}_λ belongs to one of the solution sets of $S_{\alpha\beta}$. If $\{\vec{P}_\beta\} \neq \{\vec{P}_\lambda\}$, then $\{\vec{P}_\alpha, \vec{P}_{\alpha+1}, \dots, \vec{P}_\lambda\}$ can meet the constraints of $S_{\alpha\beta}$, and the optimal value is equal to $\{\vec{P}_\alpha, \vec{P}_{\alpha+1}, \dots, \vec{P}_\beta\}$. Therefore, $\{\vec{P}_\alpha, \vec{P}_{\alpha+1}, \dots, \vec{P}_\lambda\}$ is also an optimal solution set of $S_{\alpha\beta}$ which contains $\{\vec{P}_\lambda\}$.

APPENDIX C PROOF OF PROPOSITION 1

In Lemma 1, we have proven that the optimal solution of the minimum charging cost problem contains the optimal solution of its subproblem. In Lemma 2, we have proven that the overall optimal solution can be obtained by making a greedy choice in each step. Combining Lemma 1 with Lemma 2, it can be concluded that the optimal solutions of the subproblems obtained by greedy choice can be used to generate the optimal solution of the master problem. In other words, the optimal solution can be obtained by the greedy algorithm.

APPENDIX D PROOF OF PROPOSITION 2

To demonstrate this proposition, it is only required to prove that the statement “For minimum peak load problem, the globally optimal solution can be achieved by greedy algorithm” is not true. To this end, we use proof by contradiction. Assume that two vehicles arrive at different time in the period. Fig. 17 shows the respective arrival and departure times. Their maximum charging power limits are both 2, and the charging volume is $3\Delta T$.

Solving the minimum peak load problem yields the possible solution as shown in Fig. 18(a). In this case, the system peak load is 2.5. However, there is a better solution that meets the constraints where the system peak load is 2, as shown in Fig. 18(b).

Therefore, “For the minimum peak load problem, the globally optimal solution can be achieved by greedy algorithm” is false. In other words, the proposition is true.

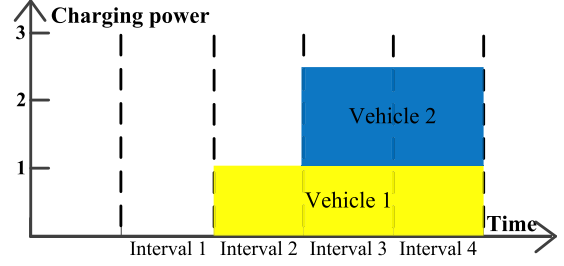


Fig. 18. Charging schedules of an example.

APPENDIX E PROOF OF PROPOSITION 3

For the network flow model, the complexity of the maximum flow algorithm is $O(VA^2)$ [28]. Since solving the network flow model requires f bisection searches, the max flow calculation is performed f times. Obviously, the complexity of the algorithm is $O(VA^2f)$. This means that such a strategy can be solved in polynomial time.

APPENDIX F PROOF OF PROPOSITION 4

By summing up Eq. (15) we have:

$$\sum_{i=1}^N D_i + \sum_{i=1}^N \sum_{j=k}^{k+m} P_{ji} \leq N \cdot L \quad (23)$$

Summing up Eq. (16) yields:

$$\sum_{j=k}^{k+m} E_j = \Delta T \times \sum_{i=1}^N \sum_{j=k}^{k+m} P_{ji}, \quad \forall j \in [k, k+m] \quad (24)$$

In essence, Eqs. (23) and (24) are the relaxation of constraints. For the minimization problem, the lower bound of the objective function can be achieved by the relaxation of constraints. Substituting Eq.(24) into Eq. (23), and eliminating the common item $\sum_{i=1}^N \sum_{j=k}^{k+m} P_{ji}$ yields:

$$\sum_{i=1}^N D_i \cdot \Delta T + \sum_{j=k}^{k+m} E_j \leq N \cdot L \cdot \Delta T \quad (25)$$

As a result, Eq. (25) can be transformed into Eq. (18).

REFERENCES

- [1] J. Timpner and L. Wolf, “Design and evaluation of charging station scheduling strategies for electric vehicles,” *IEEE Trans. Intell. Transp. Syst.*, vol. 15, no. 2, pp. 579–588, Apr. 2014.
- [2] S. Pelletier, O. Jabali, and G. Laporte, “Charge scheduling for electric freight vehicles,” *Transp. Res. Part B, Methodol.*, vol. 115, pp. 246–269, Sep. 2018.

- [3] R. A. Verzijlbergh, M. O. W. Grond, Z. Lukszo, J. G. Slootweg, and M. D. Ilic, "Network impacts and cost savings of controlled EV charging," *IEEE Trans. Smart Grid*, vol. 3, no. 3, pp. 1203–1212, Sep. 2012.
- [4] C. Maigha and M. L. Crow, "Cost-constrained dynamic optimal electric vehicle charging," *IEEE Trans. Sustain. Energy*, vol. 8, no. 2, pp. 716–724, Apr. 2017.
- [5] S. Hajforoosh, M. A. S. Masoum, and S. M. Islam, "Real-time charging coordination of plug-in electric vehicles based on hybrid fuzzy discrete particle swarm optimization," *Electr. Power Syst. Res.*, vol. 128, pp. 19–29, Nov. 2015.
- [6] W. Tang, S. Bi, and Y. J. Zhang, "Online charging scheduling algorithms of electric vehicles in smart grid: An overview," *IEEE Commun. Mag.*, vol. 54, no. 12, pp. 76–83, Dec. 2016.
- [7] J. García-Álvarez, M. A. González, and C. R. Vela, "Metaheuristics for solving a real-world electric vehicle charging scheduling problem," *Appl. Soft Comput.*, vol. 65, pp. 292–306, Apr. 2018.
- [8] D. Dallinger and M. Wietschel, "Grid integration of intermittent renewable energy sources using price-responsive plug-in electric vehicles," *Renew. Sustain. Energy Rev.*, vol. 16, no. 5, pp. 3370–3382, Jun. 2012.
- [9] L. Gan, U. Topcu, and S. H. Low, "Optimal decentralized protocol for electric vehicle charging," *IEEE Trans. Power Syst.*, vol. 28, no. 2, pp. 940–951, May 2013.
- [10] Z. Ma, D. S. Callaway, and I. A. Hiskens, "Decentralized charging control of large populations of plug-in electric vehicles," *IEEE Trans. Control Syst. Technol.*, vol. 21, no. 1, pp. 67–78, Jan. 2013.
- [11] Y. He, B. Venkatesh, and L. Guan, "Optimal scheduling for charging and discharging of electric vehicles," *IEEE Trans. Smart Grid*, vol. 3, no. 3, pp. 1095–1105, Sep. 2012.
- [12] O. Sundstrom and C. Binding, "Flexible charging optimization for electric vehicles considering distribution grid constraints," *IEEE Trans. Smart Grid*, vol. 3, no. 1, pp. 26–37, Mar. 2012.
- [13] M. F. Bandpey and K. G. Firouzjah, "Two-stage charging strategy of plug-in electric vehicles based on fuzzy control," *Comput. Oper. Res.*, vol. 96, pp. 236–243, Aug. 2018.
- [14] V. Robu, E. H. Gerding, S. Stein, D. C. Parkes, A. Rogers, and N. R. Jennings, "An online mechanism for multi-unit demand and its application to plug-in hybrid electric vehicle charging," *J. Artif. Intell. Res.*, vol. 48, pp. 175–230, Oct. 2013.
- [15] L. Jian, Y. Zheng, and Z. Shao, "High efficient valley-filling strategy for centralized coordinated charging of large-scale electric vehicles," *Appl. Energy*, vol. 186, pp. 46–55, Jan. 2017.
- [16] B. Alinia, M. H. Hajiesmaili, and N. Crespi, "Online EV charging scheduling with on-arrival commitment," *IEEE Trans. Intell. Transp. Syst.*, vol. 20, no. 12, pp. 4524–4537, Dec. 2019.
- [17] C. Yang, W. Lou, J. Yao, and S. Xie, "On charging scheduling optimization for a wirelessly charged electric bus system," *IEEE Trans. Intell. Transp. Syst.*, vol. 19, no. 6, pp. 1814–1826, Jun. 2018.
- [18] T. Zhang, W. Chen, Z. Han, and Z. Cao, "Charging scheduling of electric vehicles with local renewable energy under uncertain electric vehicle arrival and grid power price," *IEEE Trans. Veh. Technol.*, vol. 63, no. 6, pp. 2600–2612, Jul. 2014.
- [19] M. Ammous, S. Belakaria, S. Sorour, and A. Abdel-Rahim, "Joint delay and cost optimization of in-route charging for on-demand electric vehicles," *IEEE Trans. Intell. Vehicles*, vol. 5, no. 1, pp. 149–164, Mar. 2020.
- [20] J. Kang, S. J. Duncan, and D. N. Mavris, "Real-time scheduling techniques for electric vehicle charging in support of frequency regulation," *Proc. Comput. Sci.*, vol. 16, pp. 767–775, May 2013.
- [21] A. Zakariazadeh, S. Jadid, and P. Siano, "Multi-objective scheduling of electric vehicles in smart distribution system," *Energy Convers. Manage.*, vol. 79, pp. 43–53, Mar. 2014.
- [22] K. Zhan, Z. Hu, Y. Song, N. Lu, Z. Xu, and L. Jia, "A probability transition matrix based decentralized electric vehicle charging method for load valley filling," *Electr. Power Syst. Res.*, vol. 125, pp. 1–7, Aug. 2015.
- [23] H. Wu, G. K.-H. Pang, K. L. Choy, and H. Y. Lam, "A charging-scheme decision model for electric vehicle battery swapping station using varied population evolutionary algorithms," *Appl. Soft Comput.*, vol. 61, pp. 905–920, Dec. 2017.
- [24] Y. Zhang, P. You, and L. Cai, "Optimal charging scheduling by pricing for EV charging station with dual charging modes," *IEEE Trans. Intell. Transp. Syst.*, vol. 20, no. 9, pp. 3386–3396, Sep. 2019.
- [25] Z. Darabi and M. Ferdowsi, "Plug-in hybrid electric vehicles: Charging load profile extraction based on transportation data," in *Proc. IEEE Power Energy Soc. Gen. Meeting*, Jul. 2011, pp. 1–8.
- [26] Y. Cao and N. Wang, "Toward efficient electric-vehicle charging using VANET-based information dissemination," *IEEE Trans. Veh. Technol.*, vol. 66, no. 4, pp. 2886–2901, Apr. 2017.
- [27] G. M. Fetene, G. Hirte, S. Kaplan, C. G. Prato, and S. Tscharaktschiew, "The economics of workplace charging," *Transp. Res. Part B, Methodol.*, vol. 88, pp. 93–118, Jun. 2016.
- [28] T. H. Cormen, *Introduction to Algorithms*, 3rd ed. Cambridge, MA, USA: MIT, 2009.

Weitiao Wu received the Ph.D. degree in transportation engineering from the South China University of Technology, Guangzhou, China, in 2015. He is currently an Associate Professor with the South China University of Technology. His research interests include transportation electrification, public transport, traffic simulation, and optimization.



Yue Lin is currently pursuing the master's degree with the School of Civil Engineering and Transportation, South China University of Technology, Guangzhou, China. His research interests include data mining and transportation electrification.



Ronghui Liu received the B.Sc. degree from Peking University, China, and the Ph.D. degree from Cambridge University, U.K. She is currently a Professor with the Institute for Transport Studies, University of Leeds, U.K. Her main research interest includes developing traffic micro-simulation models to analyze the dynamic and complex travel behavior and interactions in transport networks.



Yaohui Li is currently pursuing the master's degree in transportation engineering with the South China University of Technology, Guangzhou, China. His research interests include traffic simulation and transportation electrification.



Yi Zhang received the B.Sc. degree from the South China University of Technology, Guangzhou, China. Her research interests include traffic simulation and artificial intelligence.



Changxi Ma received the Ph.D. degree in transportation planning and management from Lanzhou Jiaotong University in 2013. He is currently a Professor with Lanzhou Jiaotong University. He has authored three books and over 100 articles. His research interests include ITS, traffic safety, and transportation optimization.

